FLOW MEASUREMENTS DOWNSTREAM OF AN AXIAL FLOW FAN INSIDE AN OUTDOOR AIR CONDITIONING UNIT

A.R Abu Talib[1], A.A Jaafar[1], N.A Abdul Jalil[2] and A.S Mokhtar[1]
[1]Department of Aerospace Engineering, Universiti Putra Malaysia, 43400, Serdang, Selangor, Malaysia
[2]Dept. of Mechanical and Manufacturing Engineering, Universiti Putra Malaysia, 43400 Selangor, Malaysia
Email: abrahim@eng.upm.edu.my

ABSTRACT

This paper presents detailed flow measurements downstream of an axial flow fan inside an outdoor air condensing unit. The authors have successfully measured the velocity distributions at different rotational speeds using a constant temperature anemometry probe. Experiments were conducted at the Aerodynamics and Fluid Mechanics laboratory, Department of Aerospace Engineering, UPM. Flow visualisation was conducted at various positions downstream of the orifice using a particle image velocimetry system. Low velocity region was observed in the core region of the flow field. The diameter of the core flow reduces as the flow move downstream from the orifice similar to a cone shape. The behaviour of the complex flow field from the outdoor condensing unit has been successfully studied and identified. The velocity profile data will assist design engineer in the performance improvement and new design of fan blades.

Keywords: *velocity measurements, axial flow fan, constant temperature anamometer.*

INTRODUCTION

Throughout the history, the axial flow fan has been widely studied by many researchers in the world. For instance, Eck [1] defined many geometric parameters and did an extensive systematic analysis to improve the capability to evaluate fan performance. Ronald [2] has patented an apparatus for improving axial velocity profile of axial flow fans. The coupled theory of the fan and duct designs for an air moving system were developed by Wallis [3] while Yen and Lin [4] studied the exit flow field and performance of axial flow fans.

Many of the researchers are now focussing their work on the flow field between the blades due to the high unsteadiness in the axial flow fan. This unsteadiness is induced by the velocity fluctuation when the flow passes through the small gaps between the blades, plus with the existence of fan mounting. Estevadeordal et al. [5] studied the characteristics of a flow in a low speed axial fan using digital particle image velocimetry. Meanwhile, Gerald et al. [6] conducted an experimental investigation of the 3D unsteady flow field downstream of axial fans. Many techniques have been developed to visualise flow fields, such as liquid crystal techniques, schlieren photography, interferometry and the use of shadowgraphs [7 – 9]. In this study, the evidence of unsteadiness and fluctuation flow is clear and makes it difficult for the flow field to be measured by our PIV due to its limitations at the time of experimental work in our laboratory. Because of this constraint, our work shifted from PIV to CTA.

Generally, they are three kind of velocimetry that usually been used for the flowf ield measurement: (i) hot wire anemometry (CTA), (ii) laser doppler velocimetry (LDV), and (iii) particle image velocimetry (PIV). However, for the purpose of this paper, and for a better understanding of the results of this study, only brief principles for the CTA and PIV are described.

Particle Image Velocimetry (PIV)

Particle Image Velocimetry (PIV) is a whole-flow-field technique providing instantaneous velocity vector measurements in a cross-section of a flow. Two velocity components are measured, but use of a stereoscopic approach permits all three velocity components to be recorded, resulting in instantaneous 3D velocity vectors for the whole area. The use of modern CCD cameras and dedicated computing hardware, results in real-time velocity maps.

Principles of PIV

In PIV, the velocity vectors are derived from sub-sections of the target area of the particle-seeded flow by measuring the movement of particles between two light pulses. The flow is illuminated in the target area with a light sheet. The camera lens images the target area onto the CCD array of a digital camera. The CCD is able to capture each light pulse in separate image frames. Once a sequence of two light pulses is recorded, the images are divided into small subsections called inter-rogation areas (IA). The interrogation areas from each image frame, I_1 and I_2, are cross-correlated with each other, pixel by pixel. A velocity vector map over the whole target area is obtained by repeating the cross-correlation for each interrogation area over the two image frames captured by the CCD camera.

In short the technique is non-intrusive and measures the velocities of micron-sized particles following the flow, capable of measuring velocity range from zero to supersonic, instantaneous velocity vector maps in a cross-section of the flow. Results are similar to computational fluid dynamics, i.e. large eddy simulations, and real-time velocity maps are an invaluable tool for fluid dynamics researchers.

Constant Temperature Anemometry (CTA)

CTA is a point-measuring technique appropriate for the measurement of time series in 1, 2 or 3-dimensional gas and liquid flows and particularly suitable for the measurement of flows with very fast fluctuations at a point (high turbulence) and the study of flow micro structures, where there is a need to resolve small flow eddies down to the order of tenths of a mm. The CTA measures velocity at a point and provides continuous velocity time series, which can be processed into amplitude and time-domain statistics. Examples are mean velocity, turbulence intensity, higher order moments, auto-correlations and power spectra. The working principle is based on the cooling effect of a flow on a heated body.

Principles of CTA

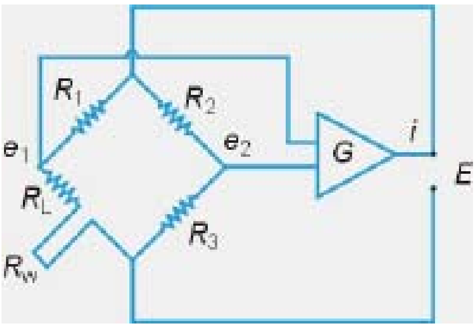

Figure 1: Wheatstone bridge

The wire, R_w, is connected to one arm of a Wheatstone bridge and heated by an electrical current (Figure 1). A servo amplifier keeps the bridge in balance by controlling the current to the sensor so that the resistance - and hence temperature - is kept constant, independent of the cooling imposed by the fluid. The bridge voltage, E, represents the heat transfer and is thus a direct measure of the velocity. The combination of the sensor's low thermal inertia and the high gain of the servo loop amplifier give a very fast response to fluctuations in the flow. CTA probes normally have tungsten wire sensors, 1 mm long and 5 mm in diameter, mounted on two needle-shaped prongs. They are available with 1, 2 and 3 wires (Figure 2). Film probes with thin-film sensors are recommended for liquid flows.

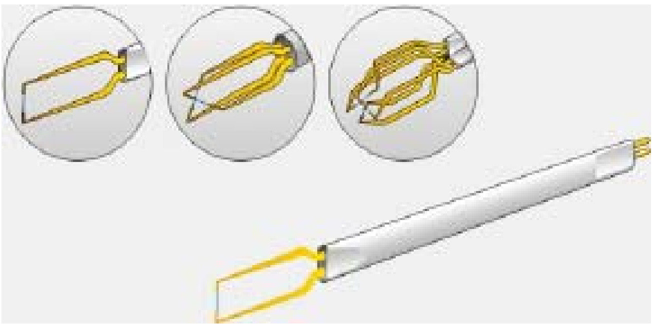
Figure 2: Samples of CTA wire probe

EXPERIMENTAL SETUP

Velocity measurements were performed using a constant temperature anemometry system from Dantec Dynamics [10]. A single wire 55P11 probe with long probe support and 4 m cable was placed on Dantec 30 kg traverse positioning system. Ideally the probe must be facing the opposite direction of the main flow. Measurements were made for a series of two-dimensional planes.

The test rig (condensing unit) is placed on a table of 0.8 m height from the ground level. To eliminate the wall effect on the flow downstream of the orifice, the test rig is placed and position such that the plane of the orifice is approximately at the edge of the table. The probe assembly and the traverse positioning system are placed in front of the orifice. The probe and 4 mm probe support hold by a probe holder which create a stem approximately 120 mm downstream from the probe, protrudes in the main flow. The plane of measurements is located approximately 330 mm from the 250 mm x 420 mm cross sectional area traverse positioning system.

Calibration

Flow calibration was carried out using Dantec Streamline Calibrator and Data Acquisition Software. The calibrations were performed from 0 to 10 m.s^{-1} and the calibration curve for ambient temperature of 31.25°C is shown in Figure 3 [11].

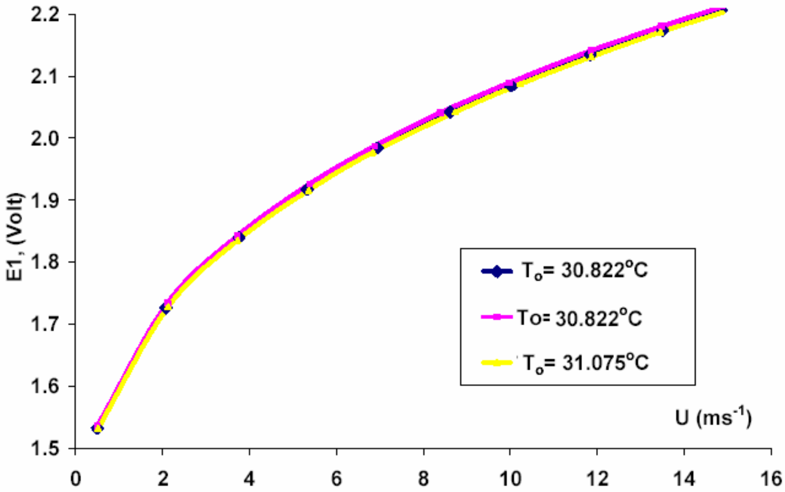

Figure 3: Calibration curve

For this intended velocity range, the manufacturer-listed accuracy for flow calibrator is ± 1% and ± 0.2% of the reading value of average velocity and turbulence intensity respectively. Three different temperature values, covering approximately 1°C range in the flow calibrator were examined. It is shown that the calibration data is virtually identical.

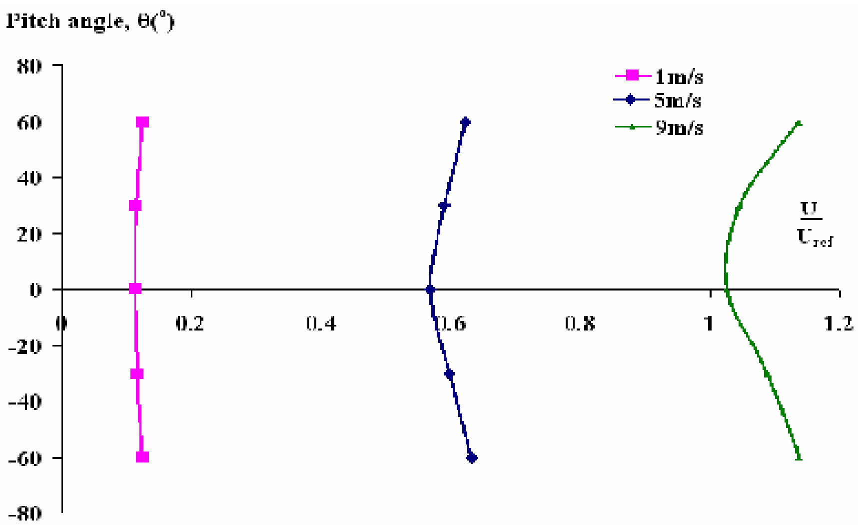

Figure 4: Effects of varying the pitch angle of the probe on average velocity of U = 1 to 9 m.s^{-1}

Figures 4-6 show the effects of probe alignment on the flow emitted from the Streamline Flow Calibrator. It is shown that the magnitude of error is increasing at higher average velocity. The following figure is the error distribution for the effect of pitching the probe. It can be shown that the error of 1% of reading value can be obtained if the probe is pitched less than 10° in the main flow. Uncertainty analysis shows that a weak effects of increasing the pitching of the probe on the uncertainty of the measured average velocity.

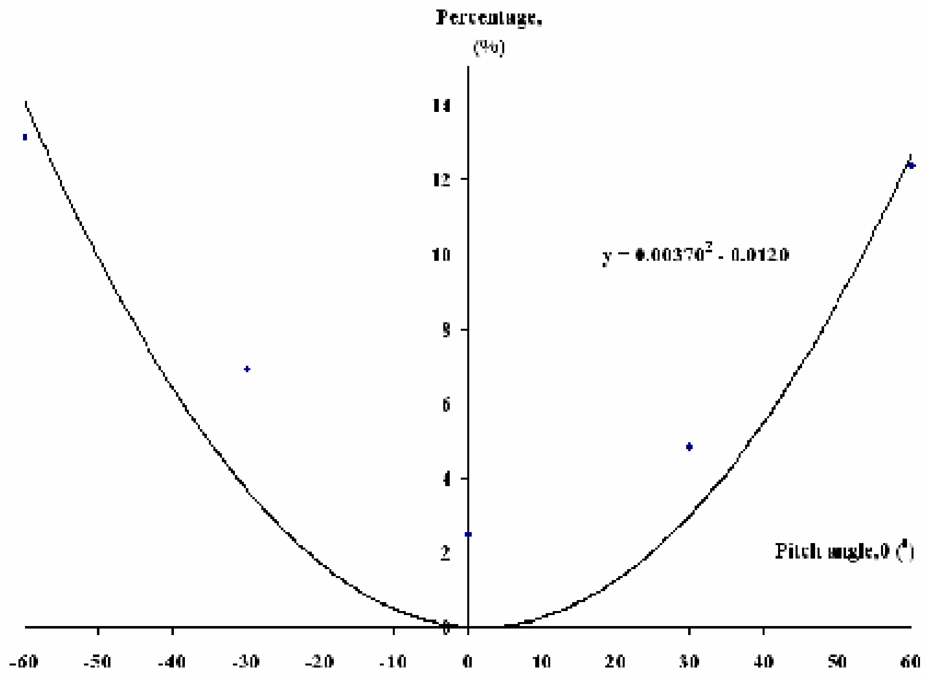

Figure 5: Percentage of error due to pitching the probe at U = 1 to 9 m.s⁻¹

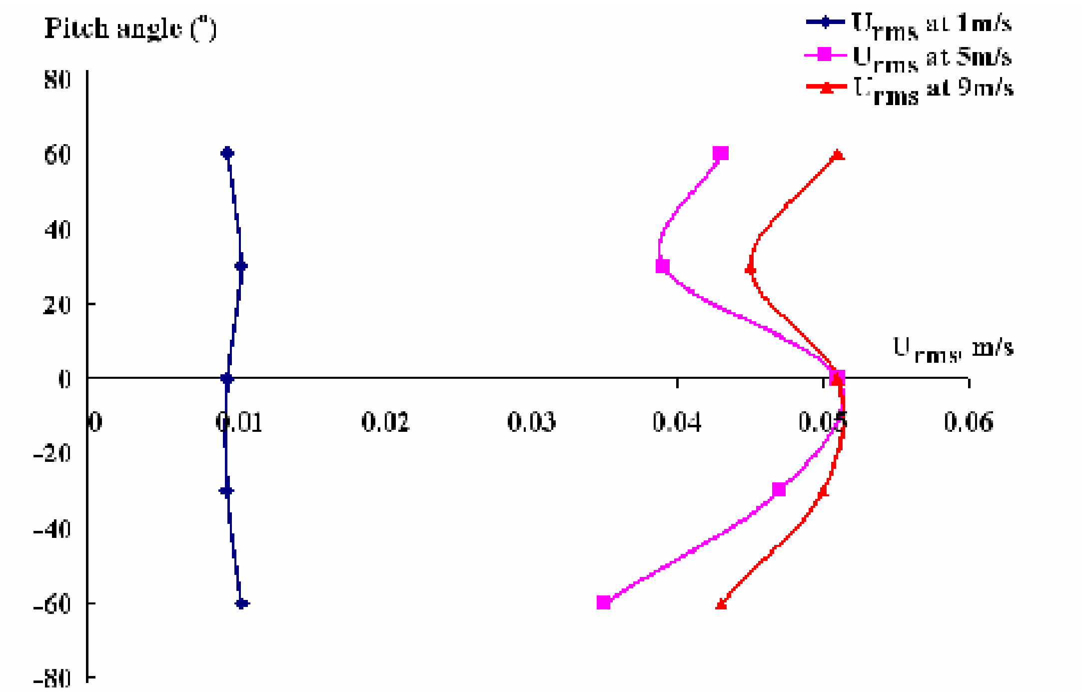

Figure 6: Effects of pitching the probe on the standard deviation

Measurement Procedure

The single wire 55P11 probe was mounted to 300 mm solid 5 mm cylinder using a probe holder. The probe assembly is placed in such a way that the probe and its support and the cylinder protrude in the fan flow path. The probe was remotely positioned in the measurement area of interest using Dantec traverse positioning system to reduce the positioning error. The smallest displacement of the traversing system is 1 mm, and a realistic statement of the error of the probe positioning distance is estimated to be 0.5 mm. Measurements were made for a series of two-dimensional plane, and the spatial resolutions of the measurement data is 100 x 100 measurement points per m^2, and detail of measurement locations is given in Table 1.

Table 1: Detail of measurement locations

Plane	**Area of coverage**	**Remarks**
Y - Z [420 mm (X) x 420 mm (Y)]	X/D = 0.036 -0.5 < Y/D =< 0.5 -0.5 < Z/D =< 0.5	X = 15 mm (-210 mm< Y < 210 mm) (-210 mm< Z < 210 mm)
	X/D = 0.25 -0.5 < Y/D =< 0.5 -0.5 < Z/D =< 0.5	X = 105 mm (-210 mm< Y < 210 mm) (-210 mm< Z < 210 mm)
	X/D = 0.5 -0.5 < Y/D =< 0.5 -0.5 < Z/D =< 0.5	X = 210 mm (-210 mm< Y < 210 mm) (-210 mm< Z < 210 mm)
X - Y	Z/D = 0 0.048 < X/D < 0.5 -0.5 < Y/D=< 0.5	Z = 0 (-190 mm< X < 210 mm) (-210 mm< Y < 210 mm)
X - Z	Y/D = 0 0.048 < X/D < 0.5 -0.5 < Z/D < 0.5	Y = 0 (-190 mm< X < 210 mm) (-210 mm< Z < 210 mm)

Where D is the diameter of the orifice, X is the axial distance from the orifice, Y is the lateral direction, and Z is the vertical direction.

Local average velocity, U is statistically evaluated from a sample of the corresponding local instantaneous value, u. Each sample has *n* = 500 data collected in a second which implies that the local instantaneous velocity is acquired every 0.002 sec.

The average value is calculated as follows:

$$U = \frac{\sum_{i=1}^{i=N} u_1}{N} \tag{1}$$

The uncertainty of the measured average value is given by the corresponding standard deviation defined as follows:

$$s = \frac{\sum_{i=1}^{i=N} (u_i - U)}{N-1} \tag{2}$$

The magnitude of the uncertainty implies the total error in the measurements, and it may be used to indicate the level of unsteadiness in the flow developments.

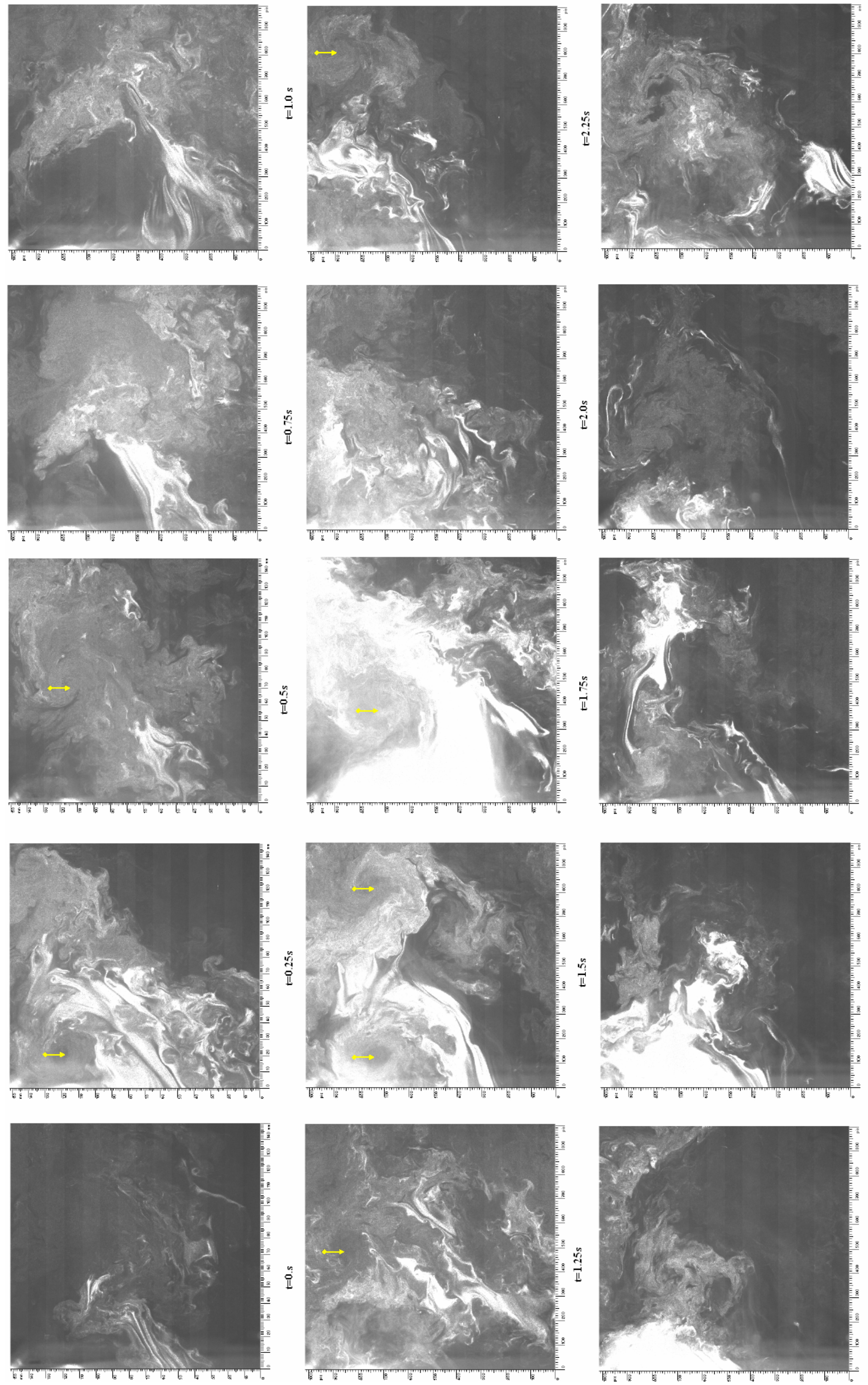

Figure 7: Sequence of images taken at 500 rpm using a Particle Image Velocimetry system

RESULTS AND DISCUSSION

Flow Visualisation

Figure 7 shows a sequence of images taken for duration of 3.5 sec using the Particle Image Velocimetry system. Images were acquired at 0.25 sec time interval for the test rig operating at 500 rpm. It is apparent that unsteady flow is developed at the downstream of the orifice plane. The unsteadiness is mainly dominated the region away from the axis of the rotations. This observation is consistent with a large standard deviation of the measured average velocity.

Flow Measurements

Flow measurements were conducted at a distance x/b = 0.25 and 0.5 for a rotational speed of 500, 600, 700 and 800 rpm as shown in Figure 8. The speed of the fan was initially set using a digital stroboscope for each of the speed required. The measurements were taken using the single wire constant anemometer wire probe at an ambient temperature of approximately 30°C. the probe was traversed in the vertical direction. Measurements were taken at 11 points at an interval of 20.5 mm apart. All of the tests were conducted in a closed ventilated laboratory to simulate the real condition operation of an outdoor condensing unit. The grill in front of the orifice was taken out during the measurements.

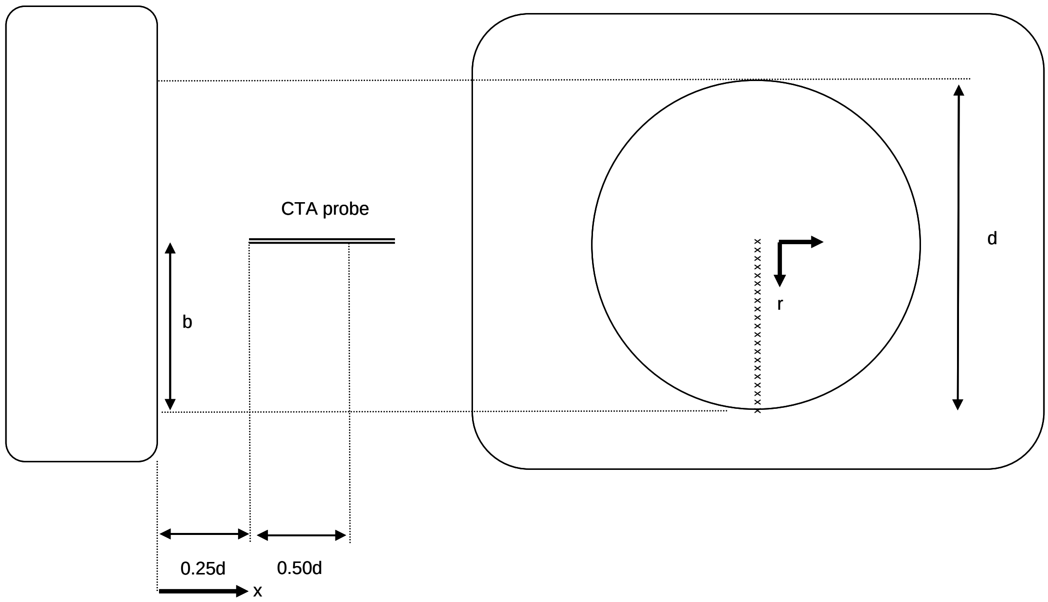

Figure 8: Schematic diagram of the plane of velocity measurements.

The results of the measured velocity profiles at x/b = 0.25 and x/b = 0.5 for speed of 500, 600, 700 and 800 rpm were displayed in Figure 9-12 respectively. Where x is the distance away from the orifice plane, b is the radius of the orifice and r is the distance from the centre of the orifice.

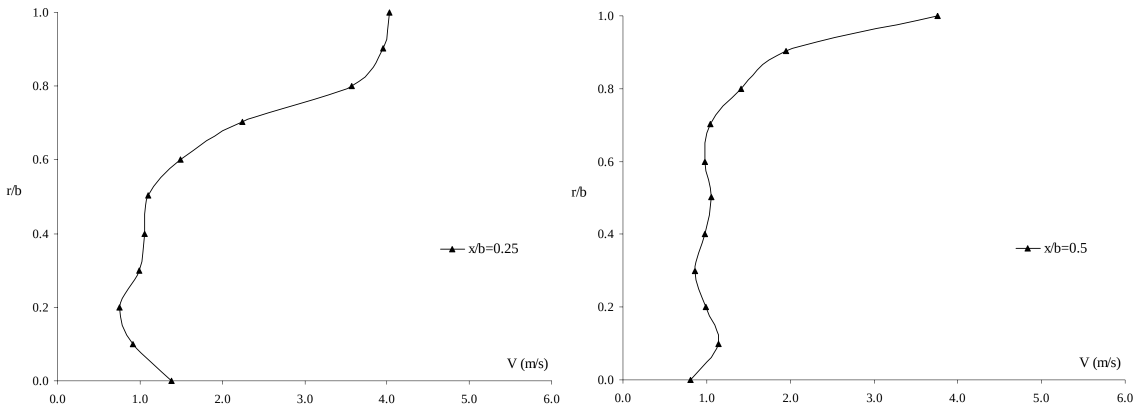

Figure 9: Measured velocity profiles at x/b=0.25 and 0.50 at 500 rpm

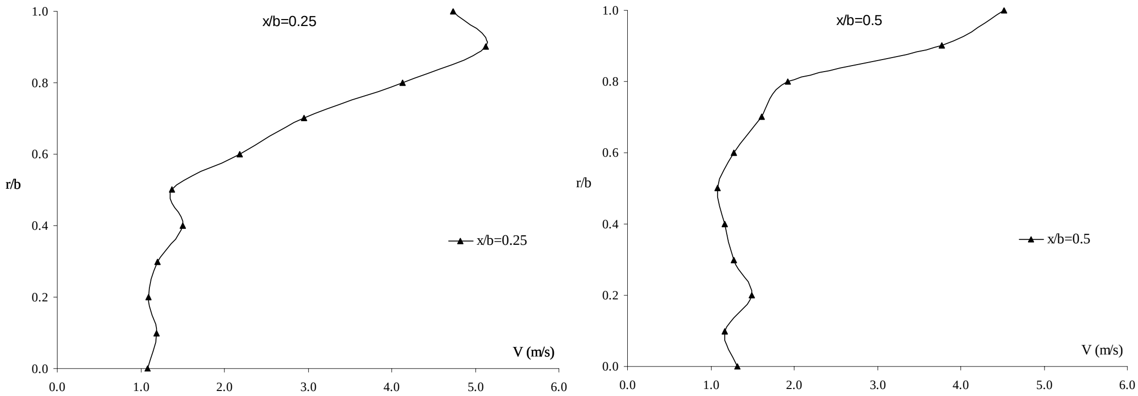

Figure 10: Measured velocity profiles at x/b=0.25 and 0.5 at 600 rpm

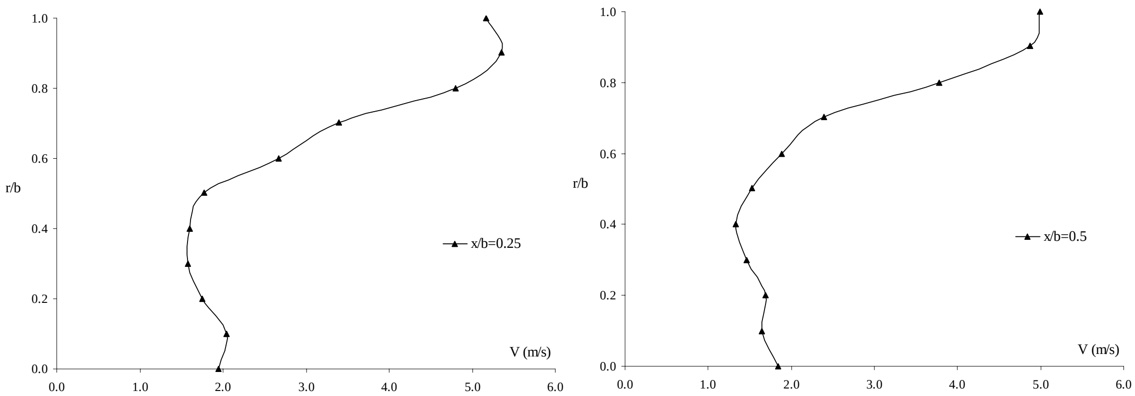

Figure 11: Measured velocity profiles at x/b=0.25 and 0.5 at 700 rpm

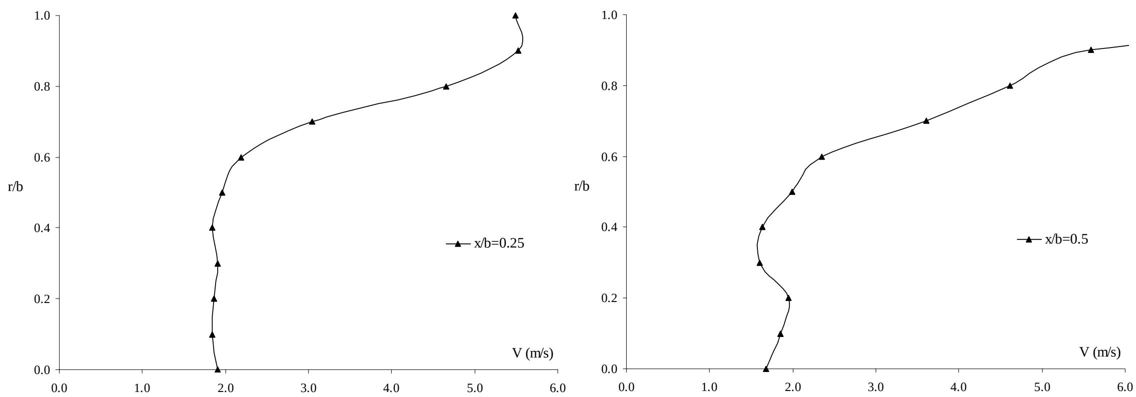

Figure 12: Measured velocity profiles at x/b=0.25 and 0.5 at 800 rpm

Detailed velocity measurements were repeated at x/b = 0.25 at 500 rpm. The measurements were conducted at a high resolution of 21 x 21 locations. The plane of measurement is shown schematically in Figure 13. However, this time the grill was placed back on the front of the orifice.

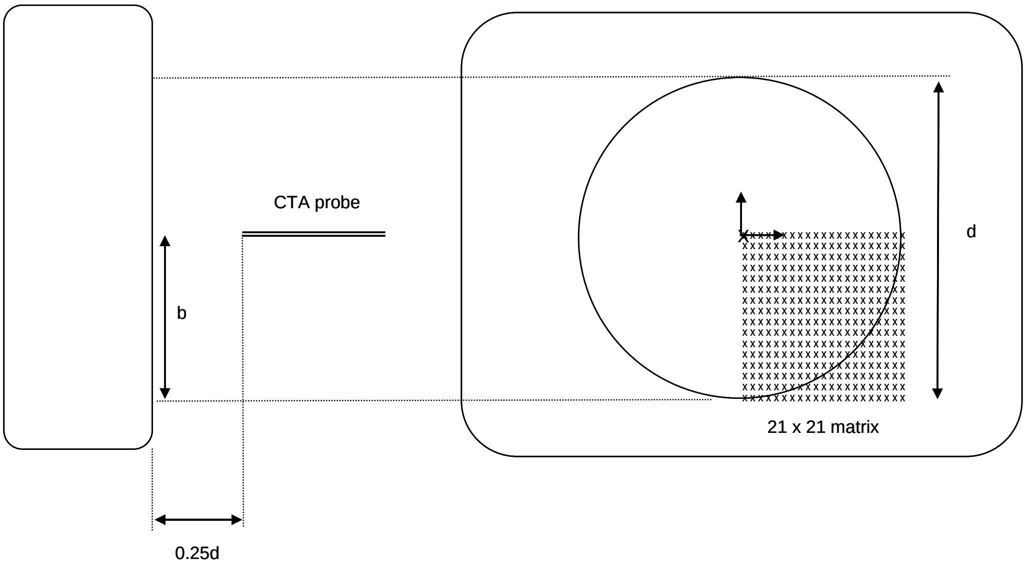

Figure 13: Schematic diagram of the plane of measurement (not to scale)

Figure 14 shows the detailed velocity distribution at x/b = 0.25 for 500 rpm. The figure shows a high velocity region near the edge of the orifice. Low velocity area was observed in the core region of the flow. The maximum velocity was found to be 3.2 m.s^{-1}.

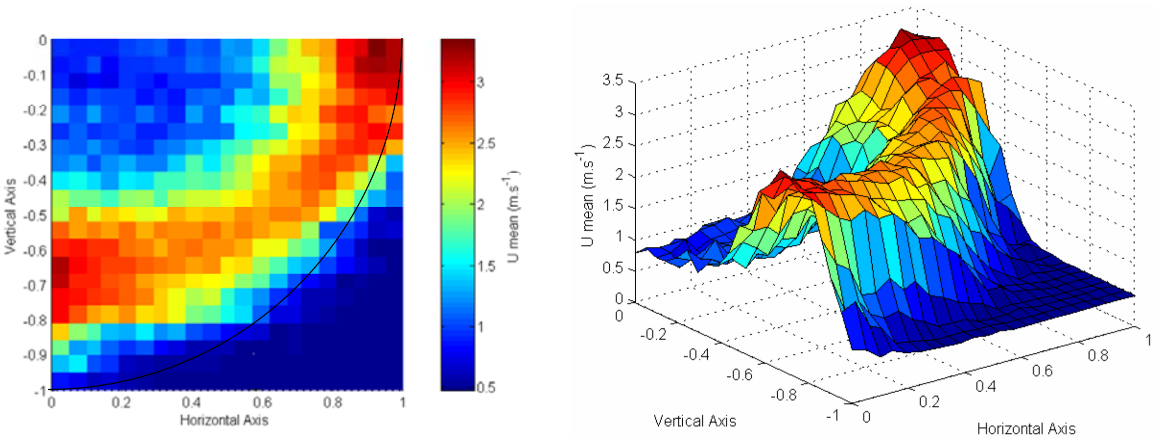

Figure 14: Detailed velocity distribution at 500 rpm (x/b = 0.25)

The average velocity profile at y = 0 and x = 0 are presented in Figure 15 and 16. Figure 17 shows the comparison of the velocity profile measured for with grill and without grill condition. It was found that both velocity profiles were approximately the same in the core region. However near the edge of the orifice the average velocity when there is no grill is approximately 25% more than when there is grill in placed.

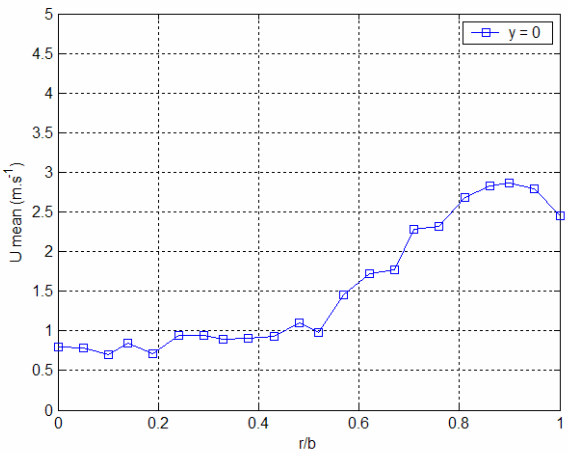

Figure 15: Average velocity profile at y = 0 (with grill)

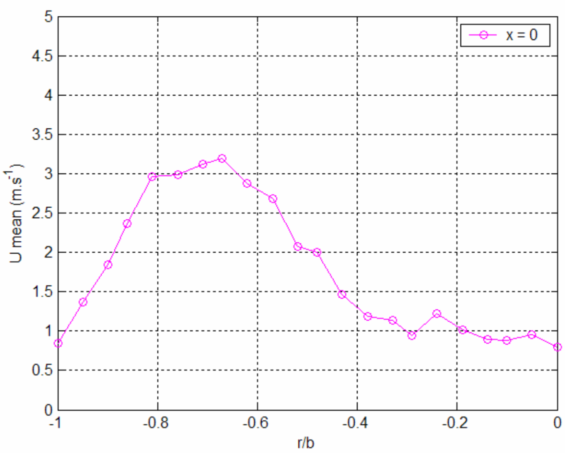

Figure 16: Average velocity profile at x = 0 (with grill)

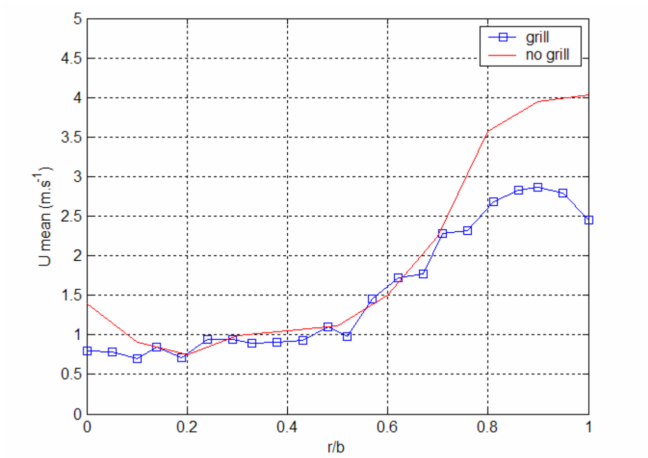

Figure 17: Average velocity profile at y = 0 (with grill and without grill)

In order to quantify the effect of the grill to the flow development downstream of the condenser unit, a full map distribution of velocity profile were needed. Two tests were conducted to measure the full distribution of the velocity profile under the 500 rpm and 700 rpm. The measurements were taken at the plane A-A, B-B, C-C and E-E. The locations of the planes are as shown in Figure 18.

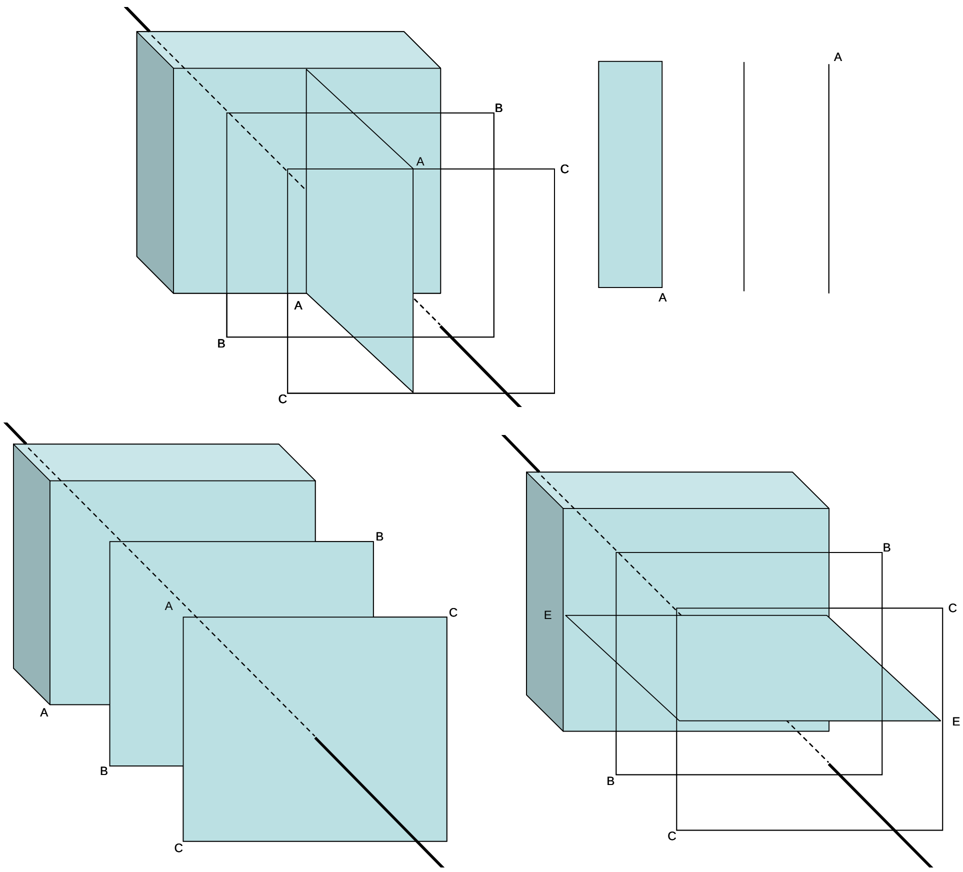

Figure 18: Schematic of the plane of measurements for A-A, B-B, C-C and E-E

Figure 19 and Figure 20 shows the full distribution of the velocity profile taken at plane A-A, B-B, C-C and E-E for 500 and 700 rpm respectively. It was observed that the core diameter of the flow reduced as the flow move away from the orifice. Uneven distribution of the velocity profiles were clearly shown in the figures. The ring shaped observed previously in Figure 14 for 500 rpm was actually an oval shape. The oval shape was also displayed in the 700 rpm test. The complex behaviour of the flow distribution from the condenser unit may possibly occur due to the design of the back casing of the condenser unit.

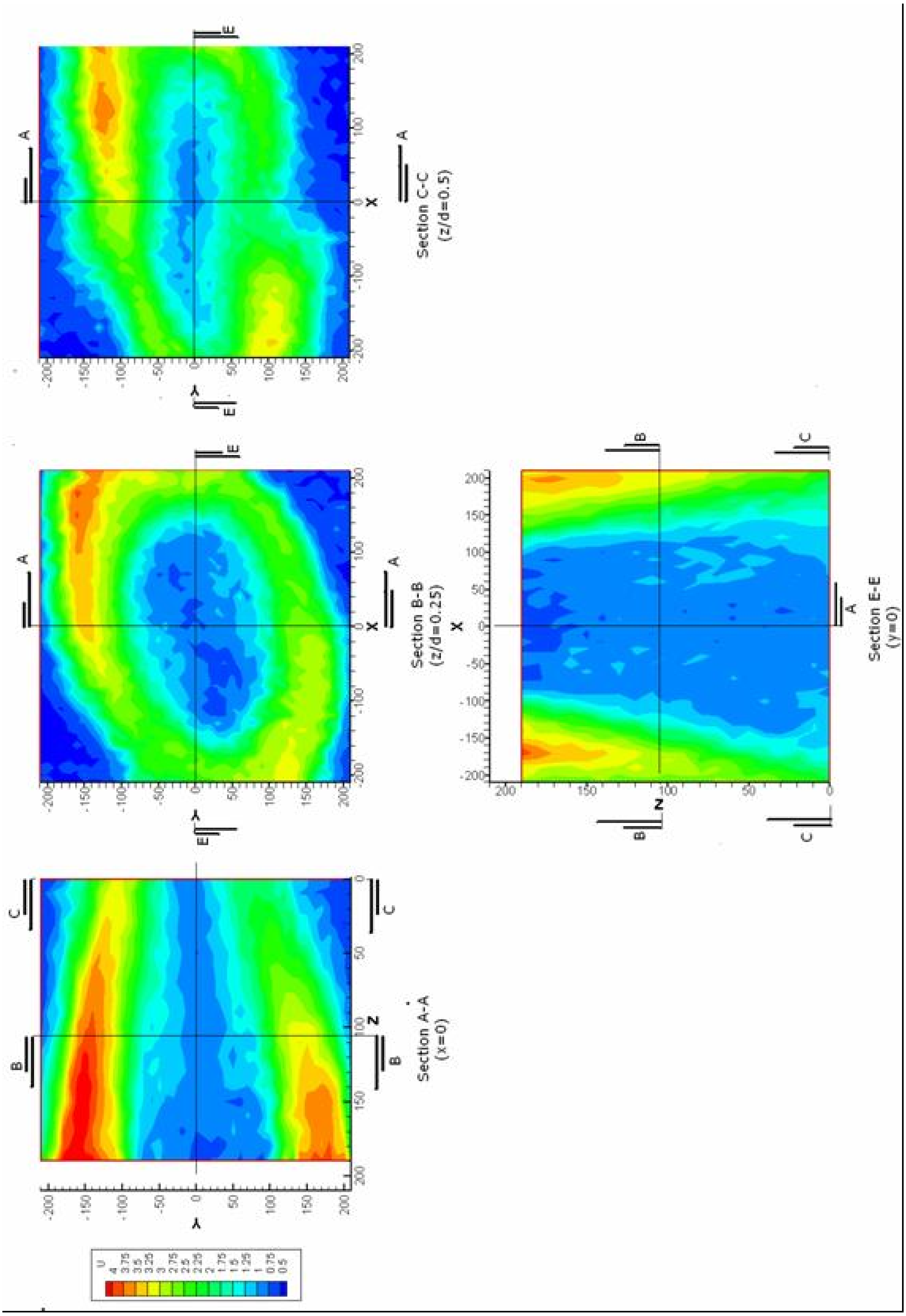

Figure 19: Full distribution of velocity profile at plane A-A, B-B, C-C and E-E for 500 rpm

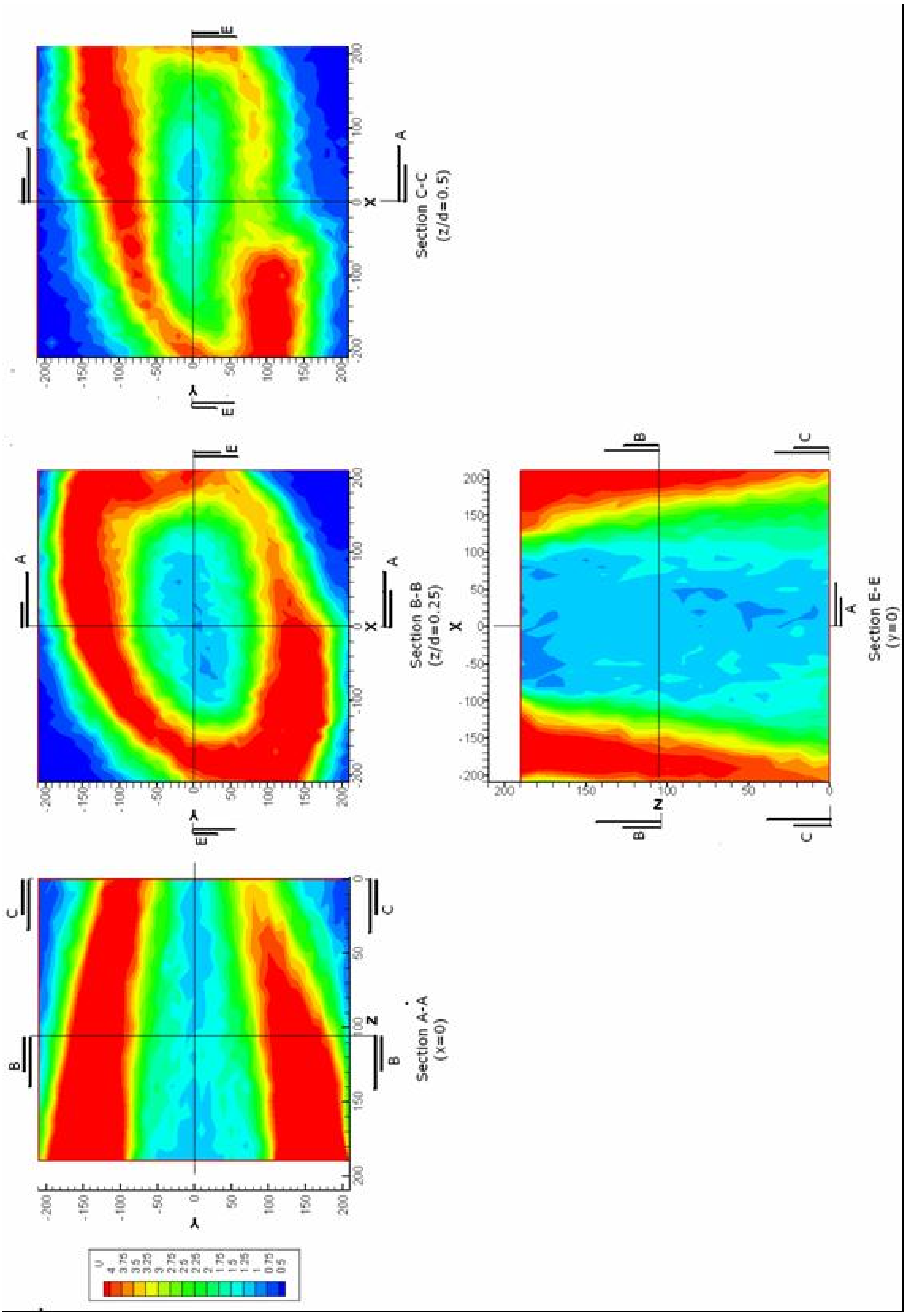

Figure 20: Full distribution of velocity profile at plane A-A, B-B, C-C and E-E for 700 rpm

CONCLUSION

Velocity measurements have been successfully measured downstream of an outdoor air condensing unit using a constant temperature anemometry probe at 500, 600, 700 and 800 rpm. Full velocity distribution map were presented at the plane A-A, B-B, C-C and E-E for 500 and 700 rpm shown an oval shape velocity level downstream of the orifice. Low velocity region can be observed in the core region of the flow field. The diameter of the core flow reduces as the flow move away from the orifice similar to a cone shape. The behaviour of the complex flow field from the outdoor condensing unit has been successfully studied and identified. This information can be incorporated in the design of new fan shape for improve performance.

ACKNOWLEDGEMENT

The authors would like to thank both Mr Onn C.C and Meng C.W from O.Y.L Research and Development Centre Sdn. Bhd., Malaysia for the research collaboration and funding of the experimental work.

REFERENCES

[1] Eck, B. (1973) *Fans: design and operation of centrifugal, axial-flow and cross-flow fans*, Azad, R.S and Scott, D.R., eds., Pergamon, Oxford.

[2] Ronald J. Lievens, (1970) Apparatus for improving axial velocity profile of axial flow fans, U.S Patent 3508842.

[3] Wallis, R.A. (1983) *Axial flow fans and ducts*, Wiley, New York.

[4] Yen, S.C., and Lin, F.K.T. (2006) Exit flow field and performance of axial flow fans, Transactions of the ASME, **128**: 332-340.

[5] Estevadeordal, J., Gogineni, S., Copenhaver, W., Bloch, G. and Brendel, M. (2000) Flow field in a low-speed axial fan: a DPIV investigation, Experimental Thermal and Fluid Science, **23**: 11-21.

[6] Gérald K., Smaïne K., Gary W.R., and Robert R, (2006) Experimental investigation of the 3D unsteady flow field downstream of axial fans, Flow Measurement and Instrumentation, **17**(5): 303-314.

[7] National Physical Laboratory (1963) Schlieren Methods, Notes on Applied Science No.31, Department of Scientific and Industrial Research, HMSO, (pp. 35-38).

[8] Kasagi, N., Moffat, R.J. and Hirata, M. (1989) *Liquid Crystals*, *Handbook of Flow Visualization*, W.J. Yang, ed., Hemisphere Publishing Corporation, (pp. 103-124).

[9] Merzkirch, W. (1997) *Flow Visualisation*, Academic Press Inc. 2nd Edition, (pp. 126-134).

[10] http://www.dantecdynamics.com/, Dantec Dynamics A/S, Tonsbakken 16-18, P.O. Box 121, DK-2740 Skovlunde, Denmark.

[11] Abu Talib, A.R., Jaafar, A.A. and Mokhtar, A.S. (2006) Flow field measurements around a propeller fan, Technical Report, Department of Aerospace Engineering, UPM, Malaysia.